Science of the Total Environment 485–486 (2014) 180–192

Contents lists available at ScienceDirect

Science of the Total Environment

journal homepage: www.elsevier.com/locate/scitotenv

A wintertime investigation of atmospheric deposition of metals and polycyclic aromatic hydrocarbons in the Athabasca Oil Sands Region, Canada

M.A. Bari [a], W.B. Kindzierski [a], S. Cho [b,*]

[a] School of Public Health, University of Alberta, Edmonton, Canada
[b] Clean Energy Branch, Policy Division, Alberta Environment and Sustainable Resource Development, Edmonton, Canada

HIGHLIGHTS

- Atmospheric bulk deposition of metals and PAH was characterized.
- Monthly sampling was carried out in winter 2012 in the oil sands region of Alberta.
- A consistent deposition pattern was observed between sites.
- The method showed the ability to obtain direct measures of wintertime deposition.

ARTICLE INFO

Article history:
Received 16 November 2013
Received in revised form 4 March 2014
Accepted 19 March 2014
Available online 12 April 2014

Editor: P. Kassomenos

Keywords:
Bulk deposition
Metals
PAH
Athabasca Oil Sands Region

ABSTRACT

With planned expansion of oil sands facilities, there is interest in being able to characterize the magnitude and extent of deposition of metals and polycyclic aromatic hydrocarbons (PAH) in the Athabasca Oil Sands Region (AOSR) of Alberta. A study was undertaken using a bulk collection system to characterize wintertime atmospheric deposition of selected inorganic and organic contaminants in the AOSR. The study was carried out from January to March 2012 at two sampling sites near (within a 20 km circle of oil sands development) and two sampling sites distant (>45 km) to oil sands development. Triplicate bulk samplers were used to estimate precision of the method at one distant site. Monthly deposition samples were analyzed for 36 metals, ultra-low mercury, and 25 PAHs (including alkylated, and parent PAH). At the two sites located within 20 km of oil sands development, 3-month wintertime integrated deposition for some priority metals, alkylated and parent PAH were higher compared to distant sites. Deposition fluxes of metals and PAH were compared to other available bulk deposition studies worldwide. Median bulk measurement uncertainties of metals and both PAH classes were 26% and within ±15%, respectively suggesting that the bulk sampling method is a potential alternative for obtaining future direct measures of wintertime metals and PAH deposition at locations without access to power in the AOSR.

1. Introduction

There has been a growing interest at the regional, provincial, national, and international levels about environmental impacts related to oil sands developments in northeastern Alberta. Alberta's oil sands are the third largest reservoir of crude oil in the world after Venezuela and Saudi Arabia, which underlie 140,200 km^2 of land in the Athabasca, Cold Lake and Peace River areas in northern Alberta (Hein et al., 2001). In 2010, Alberta's total oil reserves were about 12% of global oil reserves, i.e., 170.8 billion barrels of which crude bitumen reserves account for 169.3 billion barrels and about 80% of the reserves is considered recoverable by in-situ methods and 20% by surface mining (Alberta Energy, 2011). With increasing oil prices, planned expansion of oil sands facilities is estimated to increase production from 1.5 million barrels/day in 2010 to 3.7 million barrels/day by 2025 (CAPP, 2011).

Atmospheric deposition is a potentially important pathway of trace metals and polycyclic aromatic hydrocarbons (PAH) input to the landscape in the Athabasca Oil Sands Region (AOSR). High amounts of deposition of metals and PAH to a landscape over long periods of time (i.e., several decades or more) may lead to damage of ecosystems with little diversity (Shaw, 1987). The transfer of these pollutants from air to surface environments can occur in two ways — wet deposition (scavenging by precipitation, such as rain, snow, or fog) and dry deposition (gravitational settling) (Farmer and Wade, 1986; Bidleman, 1988; Hoff et al., 1996). The magnitude of atmospheric deposition and ratio of wet to dry deposition depend on several factors — such as emission

* Corresponding author. Tel.: +1 780 644 4717; fax: +1 780 414 6741.
E-mail address: sunhee.cho@gov.ab.ca (S. Cho).

http://dx.doi.org/10.1016/j.scitotenv.2014.03.088
0048-9697/

sources, distance to emission sources, and surface and meteorological conditions (e.g., prevailing wind directions, type, frequency and amount of precipitation) (Avila and Rodrigo, 2004; Motelay-Massei et al., 2005).

With planned expansion of oil sands development in Alberta, there is interest in being able to characterize the magnitude and extent of metals and PAH deposition in the region. Bulk (i.e., open face vessel) collection systems allow for continuous collection of wet and dry forms of atmospheric pollutants. At wet urban and rural sites where total deposition originates mainly from precipitation events, comparable results can be found for wet-only and bulk deposition methods; while at industrial sites and dry urban and rural sites, bulk deposition methods with funnel-bottle combinations are able to give a better estimate of atmospheric deposition (Gladtke et al., 2012; Aas et al., 2009; Chantara and Chunsuk, 2008). Bulk systems do not require power and have an advantage compared to wet-only systems for atmospheric deposition monitoring of particulates in remote areas because of their simplicity and cost-effective operation in large networks (Dämmgen et al., 2005; Brorström-Lunden et al., 1994; Leister and Baker, 1994; Manoli et al., 2000). We acknowledge that potential limitations of the bulk deposition method may exist. For example, bulk samplers may lead to measurement uncertainty due to flow distortion, evaporation from the open sampler, dry deposition of gases and particles through impaction and diffusion to the sampler surface (Dämmgen et al., 2005). However, others have reported that some of these effects can be considered small for measuring atmospheric deposition in remote areas distant from sources (Fowler and Cape, 1984; RGAR, 1987; Tanner, 1999; Staelens et al., 2005; Cape et al., 2009; Chantara and Chunsuk, 2008).

Numerous studies have been carried out worldwide to measure atmospheric deposition of metals (Jeffries and Snyder, 1980; Morrison et al., 1995; Azimi et al., 2003; Erisman et al., 2003; Avila and Rodrigo, 2004; Aas et al., 2009; Bacardit and Camarero, 2009; Gunawardena et al., 2013) and PAHs (Korhonen et al., 1998; Ollivon et al., 2002; Garban et al., 2002; Menichini et al., 2006; Moon et al., 2006; Motelay-Massei et al., 2007; Rossini et al., 2007; Gocht et al., 2007; Su et al., 2007; Esen et al., 2008; Wang et al., 2011; Gladtke et al., 2012; Liu et al., 2013) using bulk deposition methods. While there have been monitoring activities that relate to deposition (i.e., ambient air, snowpack, sediment and wet-only deposition), there have been no direct measurements of atmospheric bulk deposition of metals and PAH in the AOSR in the past 30 years. Only a few studies have been undertaken to characterize deposition inputs. Barrie (1980) investigated atmospheric dry deposition of trace metals during summer and performed snowpack studies during winter to characterize the fate of particulate emissions from an isolated oil sands extraction power plant on the west bank of the Athabasca River. Using snowpack sampling, Kelly et al. (2009, 2010) inferred deposition of polycyclic aromatic compounds (PACs) and 13 elements to the Athabasca River and its tributaries. A recent study (Kurek et al., 2013) inferred historical (50-year) PAH deposition using lake sediment cores to provide ecological context about oil sands development and other environmental changes affecting lake ecosystems in the AOSR. In addition, Cho et al. (2014) inferred oil sands contributions of PAH to snowpack from 108 sampling locations in the AOSR.

The AOSR is considered a large area of current interest with respect to potential deposition of trace metals and PAH. However, access to power for any type of air pollutant monitoring is lacking throughout most of the area. The study was carried out using well-established, power-free bulk deposition samplers to measure selected metals and PAH in the AOSR for a 3 month period in winter 2012. Heavy metal content of lichen has been shown to decrease further away from atmospheric emission sources (Garty, 2004). This decrease correlates with distance for airborne particles that are transported away from point emission sources for different types of activities (e.g., smelters, steelworks, generating stations, mining sites, or mixed industrial centers) at varying distances. We hypothesize this pattern to be similar for deposition of metals and PAH emitted from oil sands point emission sources in the AOSR. One objective of our study was to characterize the wintertime bulk deposition pattern of metals and PAH with respect to distance from oil sands point emission sources. We also investigated the fingerprint profile of individual metals and PAH species in deposition samples close to versus distant from oil sands point emission sources and compared our wintertime metals and PAH deposition in the AOSR with other studies worldwide. Furthermore, we characterized the emission source type that deposition samples most-likely represented using the diagnostic PAH ratio approach.

2. Methodology

2.1. Sampling strategies

The choice of sampling sites for our study was an important aspect for characterizing wintertime deposition gradient in the Alberta oil sands areas. Locations that offered relatively easy access by vehicle, in open areas and not in depressions, and away more than 100 m from tree canopies or other tall obstructions were sought. Four sampling sites were used (Fig. 1a). To determine the pattern of metals and PAH atmospheric deposition, a reference location called RL (at latitude N 57° 1.50′, longitude W 111° 33.00′) was arbitrarily identified, which is an approximate mid-point position between the Syncrude Canada Ltd. and Suncor Energy Inc. oil sands operations in the AOSR. This location is within area of about a 20–30 km diameter circle consisting of several oil sands mining and upgrading operations. A further assumption was that deposition rates for these pollutants should decrease with the increasing distance away from this area (Garty, 2004; Kelly et al., 2009; Cho et al., 2014). Approximate distances of sampling sites to the arbitrary reference location are shown in Fig. 1a.

A near site co-located adjacent to one of the Wood Buffalo Environmental Association (WBEA) air monitoring station was selected as the "WBEA/Mannix" deposition site (56° 58′ 5.7″ N, 111° 28′ 55.7″ W). This was located 7.5 km from the RL and within 60 m of the WBEA station near the Suncor Energy Inc. main plant entrance. The second near site Muskeg WSC gauge (57° 11′ 43.7″ N, 111° 34′ 28.01″ W) was located 19 km north from the reference location, 4 km east of Fort McKay and within 20 km of several oil sands developments. The remaining sites were chosen at locations that would show a decreasing spatial gradient in deposition of selected metals and PAH away from the RL. A distant site was selected to the south (56° 24′ 58.5″ N, 111° 23′ 20.6″ W), which was more than 60 km away from the reference location and about 35 km south of Fort McMurray and southwest of Highway 63. To characterize variability and precision of the bulk deposition method, the second distant site served as a quality assurance (QA) site and was chosen to the north (57° 27′ 23.6″ N, 111° 33′ 0.13″ W), which was located 48 km from the reference location. As a suggested novelty of the bulk deposition approach is that it can be used to provide a measure of direct deposition at remote locations from point sources without access to power, a distant site from oil sands point sources would be best suited to assess precision for this sampling condition. Replicate sampling equipment ($n = 3$) was deployed for both metals and PAH at this site. The four sites were chosen to show a gradient of atmospheric metal and PAH deposition as distance increases from the reference location and to fall within the range of investigated sampling sites near and distant to oil sands development as reported in other studies (Kelly et al., 2009, 2010; Kurek et al., 2013; Barrie, 1980; Cho et al., 2014).

The study was carried out from January to March 2012. Northern Alberta has a 'semi-arid' climate and receives <40 cm total precipitation (rain and snow) annually and both wet and dry deposition can be important for metals and PAH. The daily temperature, snow on ground and precipitation during sampling period in the nearby city of Fort McMurray were obtained from the national climate and weather office of the Government of Canada (www.climate.weatheroffice.gc.ca) and shown in Fig. S1. The ground was covered by snow from January to

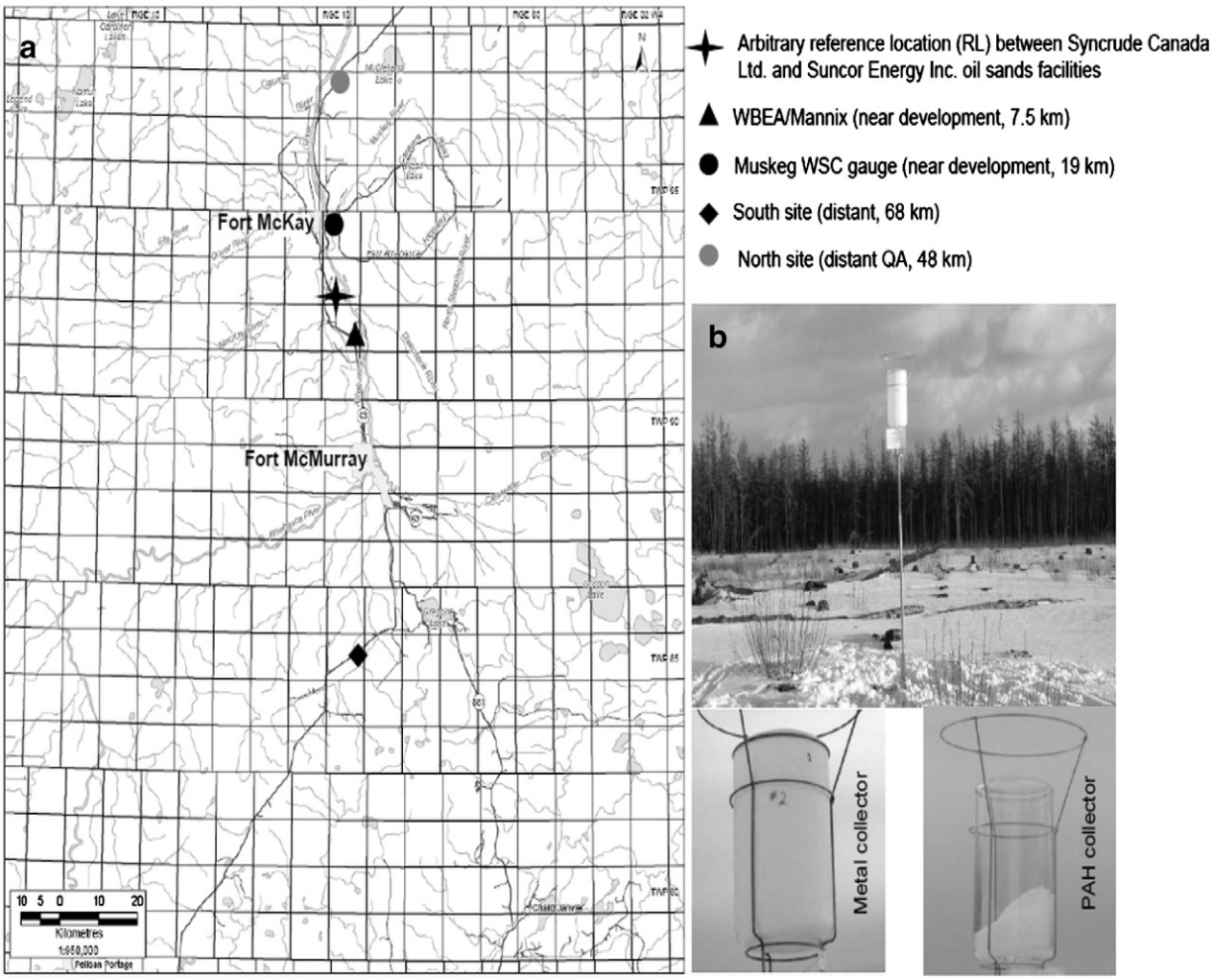

Fig. 1. Bulk deposition sampling sites in the Athabasca Oil Sands Region (AOSR) (a) and bulk deposition collectors at the north QA site (b).

March 2012 (average 26 cm) and was similar to the trend of snowfall observed for last 12 years during winter (November–April) with average snowfall ranging from 8 cm (2002) to 31 cm (2008). Average daily temperature was in the range of −31 °C to −0.7 °C from January to early March and warming days started from the middle of March. Little precipitation was observed in March and April. Bulk deposition samples were collected monthly for metal analysis using bulk deposition sampler from the Norwegian Institute for Air Research (NILU, www.niluinnovation.com). Design and development of NILU bulk samplers were based on the evaluation of similar equipment in use in European countries (Erisman et al., 2003; Aas et al., 2009) according to standards of the International Standardization Organization defined in ISO/DIS 4222.2 (ISO, 1979). During freezing conditions in winter when evaporation losses are low, open high density polyethylene (HDPE) collectors (20 cm surface diameter × 40 cm height) were used for collecting deposition samples for metal analysis. These collectors were fitted on an aluminum mounting stand at 2 m above the ground (Fig. 1b). The HDPE collectors were capped for transportation and handling. For collecting monthly deposition samples for PAH analysis, open cylindrical borosilicate glass collectors (surface diameter range 17.0 to 17.9 cm × 37 cm height) were fabricated in the glassblowing lab at the University of Alberta. For transportation and handling, glass collectors were sealed with Teflon-lined lids in conjunction with foam padded plates at the top and bottom in a screw-type aluminum frame. All collectors were safely transported by vehicle to the laboratory about 5 h away from the AOSR for analysis. Bulk deposition collectors for metals and PAH are shown in Fig. 1b.

2.2. Chemical analysis

All analyses were done at the Alberta Innovates — Technology Future laboratory in Vegreville, Alberta. Prior to sending to the field for deposition sampling of metals and PAH, HDPE and glass collectors were washed using detergent and hot water, re-washed using reverse osmosis (RO) water and rinsed using double distilled water (DDW). Leaching tests were performed on HDPE collectors for metal concentrations. HDPE collectors were soaked with 5% nitric acid for at least 24 h and rinsed with DDW as well as re-soaked with 1% nitric acid (HNO_3) for 24 h, and then the 1% nitric acid solutions were analyzed for 32 metals by inductively coupled plasma spectrometry method (ICP-MS) to check cleanliness of the collectors. Small amounts of antimony (Sb) leaching have been reported when the HDPE containers were used (Andra et al., 2012; Krachler et al., 2005). However, in this study, Sb concentrations in 6 blank tests were in the range of <0.001 to 0.003 μg/L, which are considered negligible. Glass collectors were rinsed with dichloromethane (DCM) solvent, dried, and then rinsed with DDW as well. The collectors received a final rinse with DDW, were dried, sealed with Teflon-lined lids, packed in boxes, and then transported by the lab to the field for sampling. PAH cleanliness of the collectors was proved in the lab by adding 1 L of organic free water and allowing them to soak over 72 h. The water was then extracted and analyzed for the target PAH compounds as the samples. No PAH were detected in the blank glass collectors.

Metal deposition samples were analyzed for 36 heavy and trace metals by ICP-MS (Perkin-Elmer Elan DRC-II). For determination of

extractable or total recoverable elements, samples were preserved in the lab with 1% concentrated high purity HNO_3 and allowed to stabilize for 24 h before digestion or analysis. For total recoverable metals, 40 ml of 1% HNO_3 sample solutions were digested in closed vessels under microwave heating. Since Hg results obtained from ICP-MS analysis were below detection limit at all sampling sites, the analysis of ultra-trace levels of Hg was carried out by cold vapor atomic absorption spectrometry (CV-AAS). For ultra-trace Hg analysis, 0.5% BrCl preservative was added to 100 mL sample solutions. Calibration curves were established using standard blank and 1, 10, 100 ppb multi-standard solutions, and multi-internal standard including several chemical elements such as scandium (Sc), yttrium (Y), indium (In) and holmium (Ho) was applied for ICP-MS analysis.

The isotopic dilution technique was followed for PAH extraction and clean-up. PAH deposition samples were spiked with surrogate standards at the 0.2 μg/L level. The collectors were rinsed with 100 mL of organic free water followed by approximately 50 mL DCM. The initial DCM rinse was used for the first organic extraction and two subsequent DCM aliquots of 50 mL each was used to complete the extraction. A TurboVap concentrator was used to concentrate the samples to a final volume of 1 mL. During this process, the solvent was exchanged to hexane. The 1 mL hexane extract was spiked with deuterated internal standards, to enable the use of the isotopic dilution technique for final concentration calculations. Clean-up using a 5% deactivated silica-gel (1.0 g) column was used to separate PAH components from the hexane extract. After the aliphatic fraction was eluted from the column with 3 mL of hexane, the PAH fraction was collected using 10 mL of 10%DCM/90% hexane. The resulting solvent was then concentrated to 1 mL by TurboVap. Extracts were analyzed for alkylated and parent PAH by an Agilent 5973 Gas Chromatography/Mass Selective Detector (GC/MSD) using Selective Ion Monitoring (SIM) mode, monitoring the base ion for each of the target compounds. A 30 m long capillary column HP-5MS (0.25 mm film thickness, 0.25 mm internal diameter) was used for separation. The GC temperature program was 60 °C for 1 min, 60 °C to 160 °C at 25 °C/min, 160 °C to 268 °C at 3 °C/min, 268 °C to 300 °C at 12 °C/min for 4 min, and 300 °C to 325 °C at 25C/min for 3 min with direct on-column injection using oven track mode. Multiple groups of SIM ions were used to emulate the screening conditions.

2.3. Quality assurance

To check the reproducibility and precision of the bulk deposition method, triplicate bulk samplers were used at the north QA site, which were placed within 40 m of each other in a large open, flat area. Measurement of metals and PAH requires strict precautions to prevent contamination and other sources of error. Data quality was assessed using one field blank and one trip blank, which were prepared, transported, stored and analyzed in the same way as an exposed sample in order to identify possible contamination from field operations. Before deploying sampling collectors to the field, all HDPE and glass collectors were used for blank tests. For metals, instrument detection limits or minimum reported value (MRV) were based on 3 times of standard deviations of 6 to 8 blank sample signal levels (background levels) after Currie (1995). Method detection limits (MDL) were based on duplicated digestion, duplicated determination and 1/10th concentration of the lowest standards. Analytical results were not flagged if they were below the MDL but above the MRV. The MDL for parent PAH was expected to be 0.01 μg/L and for alkylated PAH compounds at a more conservative 0.1 μg/L, and concentrations below these levels were detectable. For this study, all concentrations detected below 0.005 μg/L were represented as zero and no correction or exclusion was made for species with values below the MDL. For QA/QC of metal results, NIST standard reference materials SRM 1643e (Trace Element in Water) and SRM 1641d (mercury in water) were used. The obtained recoveries ranged from 92% for Ag to 102% for Al. For spike recoveries, 10 ppb multi-standard solution was added as a spike for one of the deposition samples and % recoveries of spike solutions ranged from 94% for Th to 109% for Al.

2.4. Data analysis

2.4.1. Bulk deposition

We defined bulk deposition flux of a chemical species as the mass transport rate per unit area. The bulk deposition flux of an element or a compound (i.e., amount deposited monthly on a 1 m^2 surface) was calculated according to Eq. (1):

$$D_{\mathrm{m}} = \frac{CV}{\pi r^2 T} \tag{1}$$

where, D_m is deposition flux of an element or a compound 'm' given in (μg/m^2/month), C is concentration in μg/L, V is the sample volume in L, r is radius of the collector surface in meter, and T is the sampling duration. We calculated and discussed bulk deposition quantities as 3-month integrated bulk deposition (μg/m^2). Monthly bulk deposition of metals (or PAH) was summed to determine the integrated (3 months) bulk deposition. For ease of comparison with other studies, daily bulk deposition flux (μg/m^2/day) was also calculated by dividing monthly deposition flux with the number of sampling days.

2.4.2. Measurement uncertainty

For quality assurance, the standard uncertainty between samplers was estimated using parallel independent bulk measurements by applying Eq. (2) according to ISO guidelines defined in EN-ISO 20988 (ISO, 2007):

$$\text{Uncertainty}, w_{bs} = \sqrt{\frac{1}{n(p-1)}\sum_{i=1}^{n}\sum_{j=1}^{p}\left(y_{i,j}-y_i\right)^2} \tag{2}$$

where $y_{i,j}$ is the observed value in period i in j measurement, y_i is the average value for period i, n is the number of parallel samples and p is the number of replicates. The relative standard uncertainty (w_{bs}%) or relative standard deviation (RSD), also known as coefficient of variation (CV) is estimated by dividing the standard uncertainty by the average concentration of all measurements.

2.4.3. Source identification

The diagnostic PAH ratio approach has been applied to characterize and qualitatively identify different emission sources that release pollutants into the environment (Sawicki, 1962). Numerous PAH deposition studies (Lian et al., 2009; Kelly et al., 2009; da Silva and Bícego, 2010; Botsou and Hatzianestis, 2012) used diagnostic ratios for source identification. It has been reported that PAH diagnostic ratios have limited applicability due to substantial intra-source variability and inter-source similarity of PAH isomer ratios arising from atmospheric processes (e.g., gas/particle partitioning), reactivity precipitation scavenging, and particle deposition (Galarneau, 2008). However, Mari et al. (2010) measured PAH congener profiles at urban and rural locations and found these profiles to be remarkably similar; suggesting that atmospheric decay processes are relatively slow for PAH (i.e., atmospheric transformations and reactions on sampling media are of relatively little importance). Their findings support using such profiles or isomer ratios to infer sources. In addition, relatively few differences in PAH profiles have been observed in distinct locations of Canada (Sanderson et al., 2004) based on investigating diagnostic ratios mostly for particle-phase PAH. In this study, diagnostic ratios were applied to the investigated bulk deposition of PAH, which is controlled mainly by particle-phase organic compounds in air (Bidleman, 1988; Cousins et al., 1999; Zhang et al., 2001; Huang et al., 2011), thereby exhibiting less volatile and semi-volatile PAH, and more particle-phase PAH.

3. Results and discussion

3.1. Quality assurance of the bulk sampling method

Uncertainty in deposition measurements can depend on several factors such as sampling protocols, analytical methods, sample preparation including transport and meteorological conditions (Aas et al., 2009). To quantify precision of the bulk sampling method, parallel independent triplicate sampling was performed at the north QA site (Fig. 1) during each month. The estimated standard uncertainty between bulk samplers is shown in Table 1. In this pilot study, the median of between sampler uncertainty (w_{bs}%) or in terms of RSD for all metals was 26% (interquartile range, IQR = 20–32%). The measurement uncertainties for As, Cd, Ni and Pb were 11–32%, which were comparable to results for similar types of NILU bulk samplers used in background stations in Finland (10–35%) as reported by Kyllönen et al. (2009), and in four different types of European sites (15–24%) as reported by Aas et al. (2009).

In our study, the median uncertainty for alkylated and parent PAH compounds were 10% (IQR = 7–11%) and 16% (IQR = 12–27%), respectively. In general, the median uncertainties were within ±15% for both PAH classes and a better apparent precision was observed for bulk deposition sampling of alkylated PAH compared to parent PAH. In our study, uncertainties of benzo(a)anthracene-BaA (26%), benzo(a)pyrene-BaP (13%), and indeno(1,2,3-cd)pyrene-IcdP (9%) were found to be lower than the bulk deposition measurements of these compounds carried out in Austria (15–120%), Germany (15–49%), France (14–50%) and the Netherlands (33–39%) using Bergerhoff open-jar collector (Gladtke et al., 2012). Our results were comparable to bulk PAH measurements using stainless steel buckets (mean RSD 12%, range 5–24%) in North China (Wang et al., 2011). Thus observed uncertainties of the bulk sampling method in the pilot study were consistent than those observed for similar studies in published literature.

3.2. Inferred deposition pattern with respect to distance from oil sands point emission sources

The pattern of observed deposition of metals and PAH at sampling sites beyond 30 km from the reference location was consistent with expected behavior for chemical species emitted to the atmosphere from industrial and other anthropogenic processes; i.e., these species should exhibit lower bulk deposition further from the sources (Garty, 2004).

Table 1
Uncertainties (μg/m^2/day) between bulk deposition samplers at the north QA site.

Metals	Average μg/m^2/day	w_{bs} μg/m^2/day	w_{bs}% or RSD (%)	Alkylated and parent PAH	Average μg/m^2/day	w_{bs} μg/m^2/day	w_{bs}% or RSD (%)
Priority metals[a]				*Alkylated PAH*			
Antimony (Sb)	0.005	0.001	26	1-Methylnaphthalene (C1-Nap)	0.008	0.0004	5
Arsenic (As)	0.03	0.01	32	2-Methylnaphthalene	0.013	0.002	17
Beryllium (Be)	0.01	0.003	31	C2-naphthalene (C2-Nap)	0.01	0.0004	4
Cadmium (Cd)	0.005	0.001	25	C3-naphthalene (C3-Nap)	0.011	0.0004	4
Chromium (Cr)	0.22	0.11	52	C4-naphthalene (C4-Nap)	0.013	0.002	14
Copper (Cu)	0.55	0.09	17	C1-fluorene (C1-Fl)	0.01	0.0001	1
Lead (Pb)	0.19	0.02	11	C2-fluorene (C2-Fl)	0.012	0.001	8
Mercury (Hg)[b]	0.65	0.2	30	C3-fluorene (C3-Fl)	0.008	0.0001	1
Nickel (Ni)	0.24	0.05	19	C4-fluorene (C4-Fl)	0.016	0.002	10
Selenium (Se)	0.02	0.001	9	C1-phenanthrene/anthracene (C1-P/A)	0.048	0.005	10
Silver (Ag)	0.002	0.001	27	C2-phenanthrene/anthracene (C2-P/A)	0.04	0.004	10
Thallium (Tl)	0.002	0.001	22	C3-phenanthrene/anthracene (C3-P/A)	0.024	0.002	8
Zinc (Zn)	1.72	0.78	46	C4-phenanthrene/anthracene (C4-P/A)	0.042	0.005	11
Other metals				C1-chrysene (C1-Chr)	0.054	0.006	11
Aluminum (Al)	96	30	31	C2-chrysene (C2-Chr)	0.039	0.003	8
Barium (Ba)	2.42	0.48	20	C3-chrysene (C3-Chr)	0.012	0.001	12
Bismuth (Bi)	0.006	0.0002	40	C4-chrysene (C4-Chr)	0.063	0.004	6
Boron (B)	0.45	0.12	28	C1-dibenzothiophene (C1-DBT)	0.04	0.004	10
Calcium (Ca)	519	83	16	C2-dibenzothiophene (C2-DBT)	0.053	0.006	11
Chlorine (Cl)	34.9	8.6	25	C3-dibenzothiophene (C3-DBT)	0.036	0.003	9
Cobalt (Co)	0.08	0.01	13	C4-dibenzothiophene (C4-DBT)	0.014	0.001	10
Iron (Fe)	210	59	23	C1-fluoranthene/pyrene (C1-F/P)	0.021	0.002	10
Lithium (Li)	0.06	0.04	54	C2-fluoranthene/pyrene (C2-F/P)	0.027	0.003	9
Magnesium (Mg)	95	19	20	C3-fluoranthene/pyrene (C3-F/P)	0.018	0.002	11
Manganese (Mn)	12.14	2.39	20	C4-fluoranthene/pyrene (C4-F/P)	0.014	0.001	7
Molybdenum (Mo)	0.02	0.007	38	*Parent PAH*			
Phosphorus (P)	11.57	5.75	50	Naphthalene (Nap)[c]	0.016	0.006	40
Potassium (K)	59	21	35	Acenaphthene (Ace)[c]	–	–	–
Silicon (Si)	184	57	31	Acenaphthylene (Acy)[c]	–	–	–
Sodium (Na)	36.3	11.5	32	Fluorene (Fl)[c]	–	–	–
Strontium (Sr)	1.02	0.18	18	Phenanthrene (Phe)[c]	0.029	0.004	12
Sulfur (S)	271	28	10	Anthracene (Ant)[c]	0.007	0.0001	2
Thorium (Th)	0.01	0.006	43	Fluoranthene (Flu)[c]	0.014	0.004	28
Tin (Sn)	0.005	0.001	27	Pyrene (Pyr)[c]	0.016	0.003	16
Titanium (Ti)	2.32	0.59	26	Chrysene (Chr)[c]	0.043	0.006	15
Uranium (U)	0.008	0.0008	11	Benzo(a)anthracene (BaA)[c]	0.017	0.004	26
Vanadium (V)	0.36	0.1	27	Benzo(b,j,k)fluoranthene (BbjkF)	0.021	0.01	46
				Benzo(a)pyrene (BaP)[c]	0.016	0.002	13
				Indeno(1,2,3-cd)pyrene (IcdP)[c]	0.017	0.001	9
				Dibenzo(ah)anthracene (DahA)[c]	0.011	0.003	24
				Benzo(ghi)perylene (BghiP)[c]	0.013	0.001	10

–, not detected.
[a] 13 U.S. EPA list of priority pollutants including CEPA toxic substances.
[b] In ng/m^2/day.
[c] ATSDR/U.S. EPA priority PAH (Agency for Toxic Substances, Disease Registry, ATSDR, 2012; United States Environmental Protection Agency, U.S. EPA, 1977).

The integrated winter deposition of some priority metals and PAH along with the distances of sampling sites to the reference location are also shown in Table 2. The relationship between deposition of metals and PAH at the sampling sites and distance of the sampling sites to the RL is shown in Fig. 2 and Fig. S2. Exponential relationships were assumed for 3-month integrated winter deposition of metals and PAH versus distance from the reference location. The exponential relationship assumes one true source at the reference location. However, this is not the case as there are multiple oil sands developments with dissimilar metals and PAH emissions associated with their operations within a 30-km distance of the reference location and the deposition trend for metals and PAH within this distance would not be expected to conform to this relationship.

For most of the metal species (e.g., As, Ni, Cr, V), exponential relationships showed a strong non-linear association with distance from the reference location explaining 79 to 94% of variation in observed winter deposition at the sampling sites, with only 6 to 21% due to unexplained factors. For Cu, a moderate non-linear association was found between distance from the reference location and 3-month deposition — explaining 56% variance and the remaining 44% due to unexplained factors. Kelly et al. (2010) indicated that metal concentration in snowpack decreased exponentially with distance from upgrading facilities in the AOSR using snowpack sampling and they presented concentration versus distance curves for Cu and Pb. If we assume that their results conform to the same 'starting' RL as our study, Kelly et al. (2010) snow deposition patterns for Cu (and Pb) at a distance 50 away from RL would range from 1.0 μg/m^2 to 80 μg/m^2 (0.02 μg/m^2 to 30 μg/m^2). The exponential curve for wintertime 3-month integrated deposition in our bulk sampling study suggests 77 μg/m^2 for Cu (refer to Fig. 2) and 30 μg/m^2 for Pb (refer to Fig. S2) at 50 km away.

For all of the PAH groups and BaP, exponential relationships demonstrated a very strong non-linear association with distance from the reference location explaining ≥98% of variation in observed winter deposition at the sampling sites, with only ≤2% due to unexplained factors (Fig. 2). Although naphthalene (Nap) is predominately found in the gas phase (Bidleman et al., 1986), distance from the reference location still explained 71% of the variation in deposition with the remaining 29% due to unexplained factors. Generally, these exponential relationships should be suitable for predicting wintertime (3-month) deposition for other north-south locations in the AOSR versus distance from the reference location because these relationships satisfactorily explain greater than two-thirds of the variance in 3-month integrated metals and PAH deposition. The observed deposition trends of metals and PAH in this study were consistent with previous findings from lichen samples in the AOSR region (Studabaker et al., 2012; Landis et al., 2012).

3.3. Deposition profiles and comparisons with other studies

3.3.1. Atmospheric metal deposition

Winter integrated (January–March 2012) and average monthly depositions of 36 metals in the AOSR sites are presented in Table 3. Deposition amounts were found higher near oil sands developments (i.e., Mannix and Muskeg WSC gauge sites) compared to distant (i.e., south and north QA) sites, which are more than 45 km away from the oil sands developments. Out of 13 elements (Ag, As, Be, Cd, Cr, Cu, Pb, Hg, Ni, Sb, Se, Tl, Zn) considered as priority pollutants under U.S. Environmental Protection Agency (U.S. EPA) and the list of substances (As, Pb, Hg, Cd, Ni) defined by Health Canada under the Canadian Environmental Protection Act (CEPA, 1999), the most abundant trace metal in bulk deposition samples was Zn at sampling the site closest to oil sands development, followed in the order of magnitude by Cu > Ni > Pb > Cr > As > Sb > Be > Cd > Tl > Ag > Hg at the WBEA/Mannix site.

Deposition of Se was below the detection limit at the two distant (south and north QA) sites and deposition of Ag, Ti and Cd was observed to be low at all sites. At the two sites located within 20 km of major oil sands facilities, 3-month integrated deposition for metals was higher — ranging from 10- to 13-fold (As), 3- to 7-fold (Cu), 5- to 8-fold (Ni), 4- to 17-fold (Cr), and 3- to 14-fold (Sb) compared to the distant sites. In a previous study Kelly et al. (2010) conducted snowpack sampling in the AOSR region and reported that mean inferred deposition of Ag, As, Be, Cu, Cr, Pb, Zn and Hg was up to 30-fold greater within 50 km of oil sands developments than at background sties >50 km away. In our study, deposition of a few priority (e.g., As, Be, Ni, Cr, Pb, Tl) and other metals was higher at the Muskeg WSC site (19 km from RL) compared to WBEA/Mannix site (7.5 km from RL). As both of these sites are near oil sands development (at varying distances) with sources that have dissimilar emissions, this finding is not unexpected.

Winter integrated deposition of typical trace metals for petroleum oil refineries (Khalaf et al., 1982; Pacyna et al., 1984; Nriagu and Pacyna, 1988) — i.e., V (328 μg/m^2) and Ni (193 μg/m^2) was up to 20-fold and 8-fold higher at sampling sites near oil sands development compared to distant sites. Tracers of mineral soil (e.g., Al, Ca, Mg, Si, Fe, Mn, Ti, K) and marine elements (e.g., Na, Cl) were dominant metals deposited at sampling sites near oil sands development, and they were 20- to 30-fold greater compared to the south site. These results were in the same order of magnitude with previous winter snowpack studies (Barrie, 1980; Barrie and Kovalick, 1978; Jervis et al., 1982; Kelly et al., 2010), where inferred deposition of Al, Ca, Mg, Mn and Ti was found to be higher at the Syncrude oil extraction plant and the Athabasca River and its tributaries.

Na and Cl concentrations are unlikely to represent marine aerosol sources as these sources are greater than 1100 km away from the AOSR. Instead, elevated concentrations of Na and Cl may suggest much closer sources (e.g., well within 100 km of the sampling sites) such as combustion-derived sources (Kleinman et al., 1980; Lowenthal et al., 1997). During the summer, the metals Al, Ca, Na, Cl, Mg, Si, Fe, Mn, Ti, K, and S are assumed to be predominantly from windblown dust or resuspended dust from near-field, e.g., oil sands extraction and surface mining activities (Barrie, 1980). During winter due to a greater predominance of light winds and stable weather conditions (surface inversion layers, lower atmospheric mixing height and stagnation of air masses), a low inferred

Table 2
Integrated 3-month deposition (January to March 2012) of selected metals and PAH (μg/m^2) at AOSR sampling sites.

	Latitude	Longitude	Distance (km)[a]	Dir[b]	As	Ni	Cr	Cu	Hg[c]	V	Zn	Alkylated PAH	Parent PAH	Car-PAH	BaP	Nap
Reference location	57° 1.5′ N	111° 33′ W														
WBEA/Mannix	56° 58′ 5.698″ N	111° 28′ 55.66″ W	7.5	SE	16	129	80	356	215	306	829	923	248	165	31	9.1
Muskeg WSC	57° 11′ 43.681″ N	111° 34′ 28.01″ W	19	N	23	193	185	211	516	328	639	352	78	47	7	2.4
North site	57° 27′ 23.569″ N	111° 33′ 0.13″ W	48	N	2	24	21	52	354	28	147	39	12	7	0.9	0.7
QA1	57° 27′ 24.277″ N	111° 33′ 0.86″ W	48	N	4	25	25	51	69	42	216	47	16	10	1.2	0.9
QA2	57° 27′ 24.866″ N	111° 32′ 59.37″ W	48	N	3	21	17	52	275	35	145	47	14	8	1.0	1.4
South site	56° 24′ 58.547″ N	111° 23′ 20.599″ W	68.4	S	2	24	11	111	112	16	543	13	4	2	–	1.1

–, not detected.
[a] Distance from sampling sites to reference location.
[b] Approximate direction from site to the reference location.
[c] In ng/m^2.

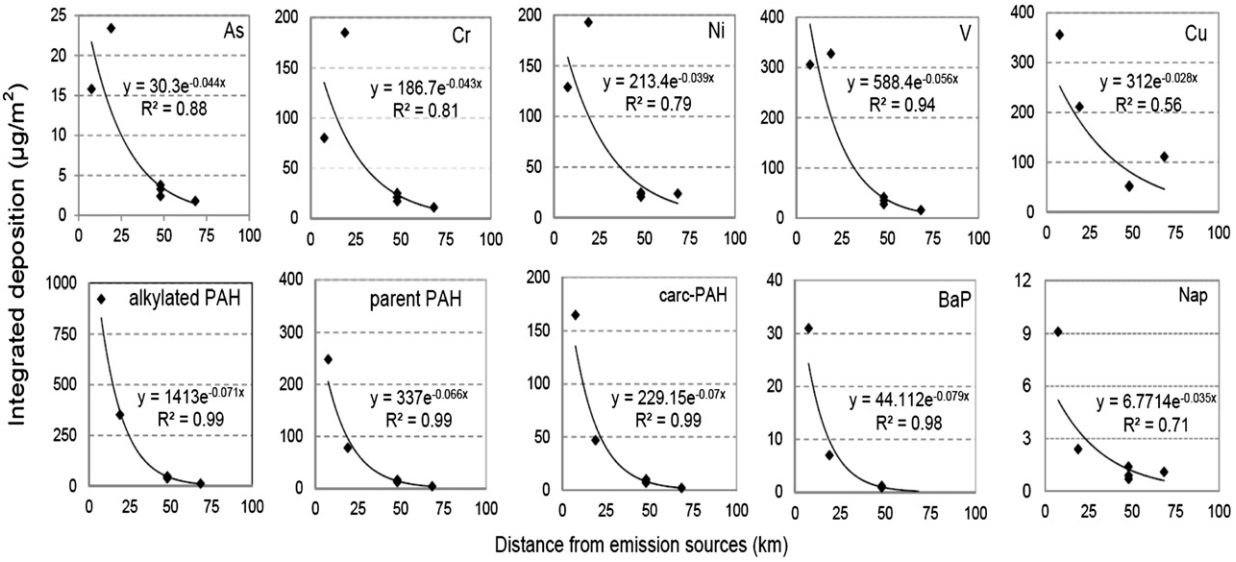

Fig. 2. Integrated 3-month (January–March 2012) winter deposition of selected metals, alkylated and parent PAH at the sampling sites versus distance from an arbitrary reference location between the Syncrude Canada Ltd. and Suncor Energy Inc. oil sands facilities.

contribution of windblown dust would be expected because of the presence of snow cover and/or wet/frozen ground conditions.

The ratios of K/Na (Oaki et al., 2002) can be used to evaluate the contribution of sea-salt (K/Na: 0.036, Thurman, 1994) and other anthropogenic sources in the urban air such as fossil fuel-type sources like oil combustion (0.09, Mizohata and Mamuro, 1980), coal combustion (0.11–0.56, Ondov et al., 1989) as well as refuse incineration (1.2–1.7, Mamane, 1988), and traffic and metal industries (1.1–4.4, Scheff and Valiozis, 1990; Huang et al., 1994). In our study, the observed ratio of 3-month integrated deposition of K/Na near oil sands development sites was greater than 0.05 and less than 0.9 (0.086 for Mannix and 0.82 for Muskeg WSC), suggesting an influence of fossil fuel combustion-derived sources.

In our study, winter deposition flux of B, Co, Mo, P, Sr, Th and U was found to be 10- to 75-fold higher at the two sites near oil sands development compared to the distant sites. Three-month integrated winter deposition of particulate Hg at the two sites near oil sands development – Muskeg WSC (516 ng/m^2) and Mannix (215 ng/m^2) – was 2- to 5-fold greater compared to the south site (112 ng/m^2). Hg can travel long distances and can be deposited far from the emission sources (Pacyna et al., 1989; Alcamo et al., 1992) as found at the north QA site (354 ng/m^2). Our integrated 3-month Hg deposition at the four sites (range: 112–516 ng/m^2) was 6 to 30 times lower than integrated 3-month wet deposition measurements carried out during winter 2008 (January–March) in downtown Toronto (~3500 ng/m^2) reported by Zhang et al. (2012).

Monthly average atmospheric bulk deposition flux of metals measured in our study was compared to other studies worldwide in Table 4. In comparing our results to other studies, we focused on bulk collection systems. Our results are only for winter season, whereas the other studies are for all four seasons so our comparison is relative only. Our intent was to try to understand whether winter deposition amounts were large relative to other studies. In general, winter deposition of As, Cr, Ni, Cu, Pb and Zn at the near development sites was found to be lower than those measured in Le Havre, France influenced by refineries and petrochemical industries (Motelay-Massei et al., 2005), in an industrial zone of Porto Marghera, Italy (Rossini et al., 2005), in urban-industrial sprawl of the Massachusetts Bay, U.S.A. (Golomb et al., 1997) and in urban sites in Belgrade, Serbia dominated by traffic and natural gas or crude oil-fired heating power plants (Mijić et al., 2010). Winter deposition flux of Mn and Fe was greater than that in other reported studies except Belgrade, Serbia. At the two distant sites in the AOSR, lower deposition flux of all metals was observed than in rural, forest and remote areas of Southern Scandinavia and England and Wales (Hovmand et al., 2008; Nicholson et al., 2003).

3.3.2. Atmospheric PAH deposition

Winter integrated (January–March 2012) deposition and average monthly and daily deposition flux of alkylated and parent PAH compounds at AOSR sampling sites are shown in Table 5. A predominance of alkylated PAH deposition was found over parent-PAH deposition at all sites. At the two sites near oil sands development (WBEA/Mannix and Muskeg WSC) integrated wintertime deposition flux values of total alkylated PAH and parent PAH were 923 and 248 µg/m^2, and 353 and 78 µg/m^2, respectively, which were up to 70-fold and 27-fold greater than at the south and north QA sites, respectively. Deposition of BaP was found to be 9- to 36-fold greater at the near sites compared to the north QA site. Deposition of all carcinogenic PAH including Nap, chrysene (Chr), BaA, benzo(b,j,k)flouranthene (BbjkF), BaP, IcdP and dibenzo(a,h) anthracene (DahA) was up to 75-fold higher at the two sites near oil sands development compared to distant sites. Although Nap has the lowest molecular mass, the highest volatility, and is present mostly in the gas phase, in our pilot study deposition of Nap was still observed up to13-fold greater at the near sites.

At sites near oil sands development, deposition flux for alkylated PAH was higher — with the maximum varying from 2.4 µg/m^2/month for C1-naphthalene (C1-Nap) to 49 µg/m^2/month for C3-fluorine (C3-Fl), 35 µg/m^2/month for C4-phenanthrene/anthracene (C4-P/A), 44 µg/m^2/month for C1-chrysene (C1-Chr), 31 µg/m^2/month for C2-dibenzothiophene (C2-DBT), and 17 µg/m^2/month for C2-fluoranthene/pyrene (C2-F/P). In contrast to this, relatively abundant parent-PAH deposition was observed with the maximum 21 µg/m^2 for Chr, 11 µg/m^2 for BaA, 12 µg/m^2 for BaP, and 6 µg/m^2 for DahA.

Among alkylated derivatives, C1–C4 chrysene homologs were the most abundant. Three-month integrated winter deposition of C1-, C2-, C3- and C4-chrysene homologs were significantly higher at the WBEA/Mannix site than at the distant sites. C1-Chr was the dominant alkyl-substituted chrysene showing a high relative content of 38% of total alkyl-chrysene series. Deposition of C1–C4 P/A was higher at sites near oil sands development than at the distant sites, where C4-P/A was abundant contributing 30 to 45% of the total P/A series. Deposition of alkylated DBT and F/P was up to 96- and 160-fold higher at the WBEA/Mannix site compared to the south site. C4-DBT and C2-F/A were dominant with a high relative content of 40% and 32% of the

Table 3
Winter 3-month integrated deposition and average deposition flux of 36 metals at the AOSR.

	3-month integrated deposition (μg/m^2)				Average deposition flux							
					Monthly (μg/m^2/month)				Daily (μg/m^2/day)			
	WBEA/Mannix	Muskeg WSC gauge	North site	South site	WBEA/Mannix	Muskeg WSC gauge	North site	South site	WBEA/Mannix	Muskeg WSC gauge	North site	South site
Distance (km)[a]	7.5	19	48	68	7.5	19	48	68	7.5	19	48	68
Priority metals[b]												
Sb	5.8	2.6	0.4	0.8	1.9	0.9	0.1	0.3	0.06	0.03	0.004	0.01
As	15.8	23.4	2.4	1.8	5.3	7.8	0.8	0.6	0.18	0.25	0.02	0.02
Be	2	6.8	0.9	0.6	0.68	2.3	0.3	0.2	0.02	0.07	0.009	0.006
Cd	1.5	1.8	0.4	0.7	0.51	0.6	0.1	0.2	0.017	0.02	0.004	0.007
Cr	80	185	21	11	27	62	7	3.6	0.9	2.01	0.22	0.12
Cu	356	211	52	111	119	70	17.4	37	3.9	2.34	0.56	1.26
Pb	70	254	22	23	24	85	7.4	7.5	0.8	2.77	0.24	0.26
Hg[c]	215	516	354	112	72	172	118	37	2.4	5.7	3.9	1.2
Ni	129	193	24	24	43	64	8	8.1	1.4	2.11	0.25	0.26
Se	2.6	0.9	–	–	0.9	0.3	–	–	0.04	0.05	0.02	0.03
Ag	0.5	0.6	0.2	0.1	0.17	0.2	0.06	0.03	0.006	0.007	0.002	0.001
Tl	0.7	2.5	0.2	0.1	0.2	0.8	0.06	0.03	0.01	0.03	0.002	0.001
Zn	829	693	147	543	277	231	49	181	9.2	7.6	1.5	5.8
Other metals												
Al	31,000	96,300	7170	4490	10,300	32,100	2390	1500	343	1050	74	50
Ba	718	1820	195	108	239	605	65	36	8	19.9	2	1.2
Bi	0.7	0.6	0.04	0.1	0.23	0.2	0.01	0.03	0.007	0.007	0.001	0.001
B	139	328	37	30	47	109	12	10	1.5	3.6	0.4	0.3
Ca	185,000	458,000	44,200	17,400	61,700	153,000	14,700	5800	2080	5150	465	195
Cl	228,000	51,600	3480	27,600	75,900	17,200	1160	9190	2540	550	36	301
Co	39	87	6.7	4.3	12.8	29	2.2	1.4	0.43	0.96	0.07	0.05
Fe	72,300	184,000	16,200	6870	24,100	61,500	5390	2290	805	2040	168	76
Li	41	143	4.4	0.3	13.7	48	1.5	0.1	0.46	1.6	0.05	0.01
Mg	40,500	103,000	8080	3780	13,500	34,200	2700	1260	455	1140	84	42
Mn	2081	6380	1070	263	694	2130	357	88	23.3	70.6	10.9	2.9
Mo	21	7.4	1.6	1.7	6.8	2.5	0.5	0.6	0.23	0.08	0.02	0.02
P	1600	4010	1090	135	532	1337	363	45	17.8	44.2	11	1.5
K	13,100	33,200	4880	2770	4360	11,100	1630	922	145	359	49	30
Si	80,000	201,000	14,100	6680	26,600	66,900	4690	2230	881	2180	144	74
Na	152,000	40,500	3860	21,200	50,700	13,500	1290	7070	1700	436	41	233
Sr	332	965	85	45	111	322	28	15.1	3.71	10.6	0.89	0.51
S	64,400	87,900	26,900	16,100	21,500	29,300	8960	5360	723	958	277	174
Th	6.6	24	0.8	0.3	2.2	8	0.3	0.1	0.07	0.27	0.009	0.004
Sn	2.6	2.5	0.8	2.4	0.9	0.8	0.3	0.8	0.03	0.03	0.008	0.03
Ti	928	2100	171	91	309	699	57	30	10.3	23.1	1.8	1
U	3.1	9.6	0.6	0.4	1.1	3.1	0.2	0.1	0.04	0.11	0.007	0.004
V	306	328	28	16	102	109	9.4	5.5	3.4	3.6	0.3	0.2

–, not detected.
[a] Distance from sampling sites to reference location.
[b] 13 U.S. EPA list of priority pollutants including CEPA toxic substances.
[c] In ng/m^2.

Table 4
Comparison of deposition flux (μg/m^2/month) of trace metals with other studies worldwide.

	Period	As	Cr	Hg	Ni	V	Cu	Pb	Mn	Zn	Fe[a]	Location	Reference
Near development sites[b]													
WBEA/Mannix	Jan.–Mar. 2012	2.2–7.1	14–37	0.02–0.12	19–45	46–183	63–189	10–33	305–1038	98–374	11–32	AOSR	This study
Muskeg WSC gauge	Jan.–Mar. 2012	5.2–11	33–80	0.08–0.26	33–92	69–150	32–128	15–174	807–3816	155–341	25–107	AOSR	This study
Distant sites[b]													
South site	Jan.–Mar. 2012	0.21–1.0	1.5–6	0.006–0.07	1.0–14	1.8–10	4.3–90	4.6–18	28–168	14–448	0.88–3.9	AOSR	This study
North site	Jan.–Mar. 2012	0.41–1.0	2.1–11	0.01–0.30	3.2–12	3.8–16	3.3–35	4.0–10.5	121–726	12.2–92	2.5–8.1	AOSR	This study
Porto Marghera, Italy[c]	1998–1999	25	102	1.7	207	240	381	228	594	2901	13	Industry	Rossini et al. (2005)
Le Havre, France[d]	2001–2002				342		783	1533		97,666		Industry	Motelay-Massei et al. (2005)
Massachusetts Bay, U.S.A.[e]	1992–1993		225		125		208	150	283	650	12	industry	Golomb et al. (1997)
Belgrade, Serbia[c]	2002–2006		135		930	1623	2835	1782	2154	3450	50	Urban	Mijić et al. (2010)
Southern Scandinavia[f]	2002–2005				25	42	83	83		575		Rural forest	Mijić et al. (2010) Hovmand et al. (2008)
England and Wales[g]	1995–1998	26	63	8.3	133		475	450		1841		Rural	Nicholson et al. (2003)

AOSR—Athabasca Oil Sands Region.
[a] mg/m^2/month.
[b] Cylindrical HDPE collector.
[c] Cylindrical PE collector.
[d] HDPE funnel-flask (weekly).
[e] HDPE bucket (wet + dry).
[f] PE funnel-flask.
[g] Frisbees-PE bottle.

total DBT and F/A series, respectively. Similarly, concentrations of alkylated Nap derivatives were higher at sites near oil sands development, where C4-naphthalene (C4-Nap) was abundant, comprising 38% of total Nap derivatives. At the near WBEA/Mannix site, the relative contribution of alkylated PAH and parent PAH was 79% and 21% of total PAH, respectively. For alkylated PAH, the four homologous series i.e., Chr (22 to 25%), DBT (14 to 20%), P/A (20 to 16%) and F/A (10 to 11%), accounted for 71 to 77% of total PAH. Similarly higher contribution of alkylated PAH was observed near oil sands development in snowpack and lake sediment studies (Kelly et al., 2009; Kurek et al., 2013; Cho et al., 2014).

Bulk deposition flux of PAH calculated as a daily average over the sampling period in our study was compared to other available bulk deposition studies worldwide (Table 6). At the near development sites, winter levels of parent-PAH (range, Mannix: 2.3–3.1 μg/m^2/day, Muskeg WSC: 0.4–1.3 μg/m^2/day) were substantially lower than those measured during winter 1991 at highly industrial sites in Manchester (range: 1.5–18.2 μg/m^2/day) and Cardiff, UK (range: 2.1–19.1 μg/m^2/day) (Halsall et al., 1997). One study conducted at an industrial site of Turkey from July 2004 to May 2005 reported bulk PAH deposition flux in winter months (January–March 2005) in the range 3.5 to 9 μg/m^2/day (Esen et al., 2008). A France study conducted between November 1999 and October 2000 at an urban site of Paris reported flux for the three winter months (January–March 2000) of 0.3 to 1.9 μg/m^2/day (Ollivon et al., 2002). In our study, winter deposition flux at the distant sites (south and north) from the oil sands development was comparable to the measurement carried out in rural areas of northern Italy from December 2003 to January 2004 (average: 0.09 μg/m^2/day, range: 0.07–0.15 μg/m^2/day) reported by Menichini et al. (2006) and in Eclaron, France conducted during March 2000 (average: 0.13 μg/m^2/day, range: 0.11–0.15 μg/m^2/day) reported by Garban et al. (2002). Another study (Wang et al., 2011) was performed in mixed environments (urban, rural, and remote) in Northern China and found substantially high deposition flux (average: 14.3 μg/m^2/day) from a 3 month (December 2007–February 2008) measurement during winter.

Although the study was of limited duration, we were able to demonstrate a clear gradient at our sites with the highest deposition at the WBEA/Mannix site (<10 km from reference location) and the lowest deposition at the distant site in the south (>65 km from reference location). Deposition ratios for alkylated PAH and parent-PAH between WBEA/Mannix site and the south site were 71:1 and 65:1, respectively. These findings demonstrated the ability of the wintertime sampling method to show a gradient at locations beyond 45 km of the reference location.

3.4. Identification of emission source type

Alkylated and parent PAH have been used to distinguish potential anthropogenic sources — e.g., pyrogenic (combustion-derived; e.g., wood combustion and vehicle emissions) and petrogenic (petroleum-derived) (Yunker et al., 1999). In general, alkylated PAH mainly originate from petrogenic sources, while parent PAH are produced from incomplete combustion of fossil fuels (Laflamme and Hites, 1978; Yunker et al., 1996). In this study, ratios of 3-month integrated alkylated/parent PAH obtained in deposition samples at the WBEA/Mannix and Muskeg WSC site were 3.7 and 4.5 respectively. The predominance of alkylated PAH over parent PAH (i.e., ratio >1.0), suggest an anthropogenic influence from petroleum-derived sources as a component of these compounds in the AOSR. The ratio of 6-ring PAH IcdP/(IcdP + BghiP) is likely to be fairly constant from emission sources to receptor location in the environment as these compounds are typically sorbed to atmospheric particles and they have similar physical and chemical properties. Yunker et al. (2002) proposed ratios of <0.2 for these compounds as suggestive of petroleum emissions, 0.2–0.5 for liquid fossil fuel combustion, and >0.5 for wood and coal combustion. In our study, IcdP/(IcdP + BghiP) ratios were 0.34 and 0.32 in deposition samples at the WBEA/Mannix and Muskeg WSC sites, respectively, suggesting an anthropogenic (fossil fuel combustion) source as a component of these compounds in deposition samples.

Alkylated PAH may vary substantially in their distribution and can be used to identify possible PAH sources. Alkylated PAH homolog series maxima at C_1 and higher indicate mature organic matter or petroleum, while a maximum at C_0 (parent PAH) usually indicates combustion (Laflamme and Hites, 1978; Wakeham et al., 1980; Sporstøl et al., 1983). The ratios of $C_0/(C_0 + C_1)$P/A and $C_0/(C_0 + C_1)$F/P i.e., the ratios of parent-PAH with mass 178 (Phe, Ant) or 202 (Flu, Pyr) to the parent-PAH plus C_1 alkylated homologs at the same mass respectively, <0.5

Table 5
Winter 3-month integrated deposition and average deposition flux of alkylated and parent PAH at the AOSR.

	3-Month integrated deposition (μg/m^2)				Average deposition flux							
					Monthly (μg/m^2/month)				Daily (μg/m^2/day)			
	WBEA/Mannix	Muskeg WSC gauge	South site	North site	WBEA/Mannix	Muskeg WSC gauge	South site	North site	WBEA/Mannix	Muskeg WSC gauge	South site	North site
C1-Nap	6.5	2.2	0.5	0.3	2.2	0.7	0.2	0.1	0.073	0.023	0.009	0.008
2-MNaP	15.1	3.8	0.8	0.3	5.0	1.3	0.3	0.1	0.17	0.04	0.01	0.01
C2-Nap	9.6	3.9	1.1	0.3	3.2	1.3	0.4	0.1	0.11	0.04	0.038	0.009
C3-Nap	8.3	2.2	–	0.3	2.8	0.7	–	0.1	0.09	0.03	–	0.01
C4-Nap	24.0	5.9	–	0.7	8.0	2.0	–	0.2	0.27	0.06	–	0.01
C1-Fl	5.9	2.7	–	0.3	2.0	0.9	–	0.1	0.06	0.03	–	0.01
C2-Fl	6.5	3.0	–	0.3	2.2	1.0	–	0.1	0.07	0.03	–	0.01
C3-Fl	55.6	8.4	–	0.3	18.5	2.8	–	0.1	0.60	0.09	–	0.01
C4-Fl	25.6	7.6	–	0.9	8.5	2.5	–	0.3	0.28	0.08	–	0.01
C1-P/A	47.6	24.0	1.1	2.7	15.9	8.0	0.4	0.9	0.53	0.26	0.01	0.04
C2-P/A	41.7	25.7	0.9	3.2	13.9	8.6	0.3	1.1	0.46	0.27	0.01	0.03
C3-P/A	14.7	11.9	–	1.4	4.9	4.0	–	0.5	0.2	0.1		0.02
C4-P/A	86.9	25.7	1.5	3.3	29.0	8.6	0.5	1.1	1.0	0.3	0.03	0.04
C1-Chr	109	34.3	2.0	4.3	36.3	11.4	0.7	1.4	1.2	0.4	0.02	0.04
C2-Chr	62.7	21.8	0.5	2.2	20.9	7.3	0.2	0.7	0.7	0.2	0.02	0.03
C3-Chr	23.3	8.7	–	0.7	7.8	2.9	–	0.2	0.26	0.09		0.01
C4-Chr	93.1	28.1	0.6	3.8	31.0	9.4	0.2	1.3	1.03	0.30	0.02	0.06
C1-DBT	52.9	18.2	0.8	2.3	17.6	6.1	0.3	0.8	0.59	0.19	0.01	0.04
C2-DBT	67.0	35.7	1.3	4.2	22.3	11.9	0.4	1.4	0.74	0.38	0.01	0.04
C3-DBT	28.8	21.1	0.3	2.0	9.6	7.0	0.1	0.7	0.32	0.23	0.01	0.03
C4-DBT	18.7	11.5	–	0.9	6.2	3.8	–	0.3	0.21	0.12		0.01
C1-F/P	30.5	9.5	0.7	1.2	10.2	3.2	0.2	0.4	0.34	0.10	0.01	0.02
C2-F/P	38.7	13.2	0.7	1.6	12.9	4.4	0.2	0.5	0.43	0.14	0.01	0.02
C3-F/P	32.0	13.6	0.2	1.0	10.7	4.5	0.1	0.3	0.36	0.15	0.01	0.02
C4-F/P	18.8	9.8	–	0.8	6.3	3.3	–	0.3	0.21	0.11		0.01
Nap	9.1	2.4	1.1	0.7	3.0	0.8	0.4	0.2	0.10	0.02	0.01	0.01
Ace	0.2	–	–	–	0.1	–	–	–	0.01	–	–	–
Acy	–	–	–	–	–	–	–	–	–	–	–	–
Fl	2.4	0.7	–	–	0.8	0.2	–	–	0.03	0.01	–	–
Phe	24.4	13.6	1.3	2.4	8.1	4.5	0.4	0.8	0.27	0.15	0.01	0.03
Ant	9.3	2.4	–	–	3.1	0.8	–	0.0	0.10	0.03	–	–
Flu	6.3	2.6	–	0.8	2.1	0.9	–	0.3	0.07	0.03	–	0.01
Pyr	19.7	5.4	0.3	0.9	6.6	1.8	0.1	0.3	0.22	0.06	0.01	0.01
Chr	54.2	19.9	0.9	2.5	18.1	6.6	0.3	0.8	0.60	0.21	0.02	0.04
BaA	27.8	6.6	0.2	0.9	9.3	2.2	0.1	0.3	0.31	0.07	0.01	0.01
BbjkF	16.8	4.6	–	1.3	5.6	1.5	–	0.4	0.19	0.07	–	0.02
BaP	31.1	7.4	–	0.9	10.4	2.5	–	0.3	0.34	0.08	–	0.01
IcdP	10.6	2.7	–	0.5	3.5	0.9	–	0.2	0.12	0.04	–	0.02
DahA	15.5	3.5	–	0.6	5.2	1.2	–	0.2	0.17	0.05	–	0.01
BghiP	20.9	5.8	–	0.9	7.0	1.9	–	0.3	0.23	0.06	–	0.01
Total alkylated PAH	923	353	13.0	39.2	307.8	117.5	4.3	13.1	10.23	3.76	0.23	0.56
Total parent PAH	248	77.6	3.8	12.3	82.7	25.9	1.3	4.1	2.76	0.88	0.06	0.18

–, not detected.

Table 6
Comparison of deposition flux (μg/m^2/day) of parent PAH with other studies worldwide.

	Period	Bulk collection system	Sampling	Parent PAH average (min–max)	Location	Reference
Near development sites						
WBEA/Mannix	January–March 2012	Cylindrical glass collector	Monthly	2.8 (2.3–3.1)	AOSR	This study
Muskeg WSC Gauge	January–March 2012	Cylindrical glass collector	Monthly	0.9 (0.4–1.3)	AOSR	This study
Distant sites						
South site	January–March 2012	Cylindrical glass collector	Monthly	0.06 (0.03–0.07)	AOSR	This study
North site	January–March 2012	Cylindrical glass collector	Monthly	0.18 (0.03–0.21)	AOSR	This study
Manchester, UK	winter 1992	Glass collector	Monthly	1.5–18.2	Industrial	Halsall et al. (1997)
Cardiff, UK	winter 1991	Glass collector	Monthly	2.1–19.1	Industrial	Halsall et al. (1997)
Bursa, Turkey	July 2004–May 2005	Stainless steel pot	Biweekly	0.3–19.5	Industrial	Esen et al. (2008)
	January–March 2005	Stainless steel pot	Biweekly	3.5–9.0	Industrial	Esen et al. (2008)
Paris, France	November 1999–October 2000	Stainless steel funnel-bottle	Biweekly	0.6 (0.2–2.0)	Urban	Ollivion et al. (2002)
	January–March 2000	Stainless steel funnel-bottle	Biweekly	0.9 (0.3–1.9)	Urban	Ollivion et al. (2002)
Southern Italy	December 2003–January 2004	Glass funnel-bottle	Monthly	0.09 (0.07–0.15)	Rural	Menichini et al. (2006)
Eclaron, France	winter 2000	Stainless steel funnel	Weekly	0.13 (0.11–0.15)	Rural	Garban et al. (2002)
Northern China	December 2007–February 2008	Stainless steel bucket	3-Month	14.3	Urban–rural-remote	Wang et al. (2011)

suggest petroleum-derived sources, while ratios >0.5 can represent combustion-derived (wood or coal) or weathered urban aerosols (Yunker et al., 2002; Simó et al., 1997). In our study, the ratios of $C_0/(C_0 + C_1)$P/A and $C_0/(C_0 + C_1)$F/P were 0.05 and 0.01 in deposition samples at the Mannix site and 0.19 and 0.05 at the Muskeg WSC site, which suggest petroleum-originated sources in the AOSR.

The ratios of dibenzothiophenes to alkylated phenanthrenes (total of all homologs or specific homologs) have been used to distinguish petroleum sources in the environment (Douglas et al., 1996; Hughes et al., 1995). A ratio of $\sum$DBT/$\sum$(P/A) >0.8 has been suggested as a potential indicator of an oil sands source (Kelly et al., 2009). In our study, the ratios of these compounds at the Mannix and Muskeg WSC sites were 0.88 and 0.99. The ratios of C3-DBT/C3-(P/A) at the near development sites were 2.0 and 1.8. Similar trends of these compounds were observed in six lake sediments (ratios ranged ~1.1–2.5, Kurek et al., 2013), in three tributaries along the Athabasca river (ratio: ~2–3, Akre et al., 2004) and eleven wetland sediments (ratio: ~1.1–1.9, Wayland et al., 2008) in the AOSR.

A component of uncertainty that is associated with the isomer ratio approach is that there is overlap in the PAH profile of multiple emission sources (Yunker et al., 2002). Consequently, PAH isomer ratios do not provide definitive identification of sources. Thus, the interpretations of diagnostic ratio results are qualitative only. To estimate relative contributions of different emission sources with greater certainty, use of multivariate source apportionment studies with long-term monitoring datasets would be necessary.

4. Summary and conclusion

Three sampling events were carried out during winter (January–March 2012) at four sites along a north-south alignment in the Athabasca river valley to quantify and characterize wintertime atmospheric deposition of selected trace metals and PAH in the AOSR. A consistent deposition pattern was observed between two sampling sites near oil sands development and two distant sampling sites (>45 km from oil sands development) for important metals (i.e., As, Ni, Cr, V) and PAH classes (alkylated, parent PAH including carcinogenic ones). Deposition observed for most metals and PAH classes conformed to expected behavior — decreasing with distance from emission sources. Sampling sites at north–south distances in excess of 45 km from oil sands development showed much smaller amounts of metals and PAH deposition compared to sites within 20 km of oil sands development. The bulk deposition method investigated in this study offers an alternative approach to obtain direct measures of wintertime metals and PAH deposition at locations without access to power and/or distant to oil sands development. We are currently considering implementing a larger scale bulk deposition study in the AOSR using additional sampling locations over multiple winters. Some of these locations would be consistent with the PAH snowpack sampling study of Cho et al. (2014).

Acknowledgment

The authors are grateful to the Government of Alberta, Alberta Environment and Sustainable Resource Development (AESRD), AMEC Environment & Infrastructure (Jane Elser, Rob Kemp) for help with fieldwork and laboratory personnel of Alberta Innovates-Technology Futures (Ryan Rybchuk, Xinbang Feng). The authors also would like to thank Lawrence Cheng and Kusumaker Sharma (AESRD) for reviewing this manuscript. This work was funded by the AESRD (AENV-POLCEP-120267) under the Comprehensive Contaminant Load Study.

Appendix A. Supplementary data

Supplementary data to this article can be found online at http://dx.doi.org/10.1016/j.scitotenv.2014.03.088.

References

Aas W, Alleman LY, Bieber E, Gladtke D, Houdret J-L, Karlsson V, et al. Comparison of methods for measuring atmospheric deposition of arsenic, cadmium, nickel and lead. J Environ Monit 2009;11:1276–83.
Agency for Toxic Substances, Disease Registry (ATSDR)http://www.atsdr.cdc.gov, 2012. [June 11, 2013].
Akre CJ, Headley JV, Conly FM, Peru KM, Kickson LC. Spatial patterns of natural polycyclic aromatic hydrocarbons in sediment in the lower Athabasca River. J Environ Sci Health A Tox Hazard Subst Environ Eng 2004;39:1163–76.
Alberta Energy. About oil sands: facts and statistics. Edmonton, Alberta: Alberta Energy; 2011 [http://www.energy.alberta.ca/OilSands/791.asp, 2011. [June 11, 2013]].
Alcamo J, Bartnicki J, Olenrzynski K, Pacyna J. Computing heavy metals in Europe's atmosphere. Model development and testing. Atmos Environ 1992;26A:3355–69.
Andra SS, Makris KC, Shine JP, Lu C. Co-leaching of brominated compounds and antimony from bottled water. Environ Inter 2012;38:45–53.
Avila A, Rodrigo A. Trace metal fluxes in bulk deposition, throughfall and stemflow at two evergreen oak stands in NE Spain subject to different exposure to the industrial environment. Atmos Environ 2004;38:171–80.
Azimi S, Ludwig A, Thévenot DR, Colin J-L. Trace metal determination in total atmospheric deposition in rural and urban areas. Sci Total Environ 2003;308:247–56.
Bacardit M, Camarero L. Fluxes of Al, Fe, Ti, Mn, Pb, Cd, Zn, Ni, Cu, and As in monthly bulk deposition over the Pyrenees (SW Europe): the influence of meteorology on the atmospheric component of trace element cycles and its implications for high mountain lakes. J Geophys Res 2009;114:G00D02. http://dx.doi.org/10.1029/2008JG000732.
Barrie LA. The fate of particulate emissions from an isolated power plant in the oil sands area of western Canada. Ann N Y Acad Sci 1980;338:434–52. http://dx.doi.org/10.1111/j.1749-6632.1980.tb17138.x.
Barrie LA, Kovalick J. A wintertime investigation of the deposition of pollutants around an isolated power plant in northern Alberta. Report ARQT-4-78. Ottawa, ON: Atmospheric Environment Service, Environment Canada; 1978. p. 127.
Bidleman TF. Atmospheric processes: wet and dry deposition of organic compounds controlled by their vapor-particle partitioning. Environ Sci Technol 1988;22:361–7.
Bidleman TF, Billings WN, Foreman WT. Vapor particle partitioning of semi-volatile organic compounds—estimates from field collections. Environ Sci Technol 1986;20:1038–43.

Botsou F, Hatzianestis I. Polycyclic aromatic hydrocarbons (PAHs) in marine sediments of the Hellenic coastal zone, eastern Mediterranean: levels, sources and toxicological significance. J Soils Sediments 2012;12:265–77.

Brorström-Lunden E, Lindskog A, Mowrer J. Concentrations and fluxes of organic compounds in the atmosphere of Swedish west coast. Atmos Environ 1994;28:3605–15.

Canadian Association of Petroleum Producers (CAPP). Crude oil: forecast, markets, &pipelines. http://www.capp.ca/getdoc.aspx?DocId=190838, 2011. [September 11, 2013].

Canadian Environmental Protection Act (CEPA)http://www.ec.gc.ca/lcpe-cepa, 1999. [June 11, 2013].

Cape JN, van Dijk N, Tang YS. Measurement of dry deposition to bulk precipitation collectors using a novel flushing sampler. J Environ Monit 2009;11:353–8.

Chantara S, Chunsuk N. Comparison of wet-only and bulk deposition at Chiang Mai (Thailand) based on rainwater chemical composition. Atmos Environ 2008;42:5511–8.

Cho S, Sharma K, Brassard BW, Hazewink R. Polycyclic aromatic hydrocarbon deposition in the snowpack of the Athabasca oil sands region of Alberta, Canada. Water Air Soil Pollut 2014;225. http://dx.doi.org/10.1007/s11270-014-1910-4.

Cousins IT, Beck AJ, Jones KC. A review of the process involved in the exchange of semivolatile organic compounds (SVOC) across the air–soil interface. Sci Total Environ 1999;228:5–24.

Currie LA. IUPAC commission on analytical nomenclature, recommendations in evaluation of analytical methods including detection and quantification capabilities. Pure Appl Chem 1995;67:1699–723.

da Silva DAM, Bícego MC. Polycyclic aromatic hydrocarbons and petroleum biomarkers in Sao Sebastiao Channel in Brazil: assessment of petroleum contamination. Mar Environ Res 2010;69:277–86.

Dämmgen U, Erisman JW, Cape JN, Grünhage L, Fowler D. Practical considerations for addressing uncertainties in monitoring bulk deposition. Environ Pollut 2005;134:535–48.

Douglas GS, Bence AE, Prince RC, McMillen SJ, Butler EL. Environmental stability of selected petroleum hydrocarbon source and weathering ratios. Environ Sci Technol 1996;30:2332–9.

Erisman JW, Mols H, Fonteijn P, Geusebroek M, Draaijers G, Bleeker A, et al. Field intercomparison of precipitation measurements performed within the framework of the Pan European Intensive Monitoring Program of EU/ICP Forest. Environ Pollut 2003;125:139–55.

Esen F, Cindoruk SS, Tasdemir Y. Bulk deposition of polycyclic aromatic hydrocarbons (PAHs) in an industrial site of Turkey. Environ Pollut 2008;152:461–7.

Farmer C, Wade T. Relationship of ambient atmospheric hydrocarbon (C12–C32) concentrations to deposition. Water Air Soil Pollut 1986;29:439–52.

Fowler D, Cape JN. The contamination of rain samples by dry deposition on rain collectors. Atmos Environ 1984;18:183–9.

Galarneau E. Source specificity and atmospheric processing of airborne PAHs: implications for source apportionment. Atmos Environ 2008;42:8139–49.

Garban B, Blanchoud H, Motelay-Massei A, Chevreuil M, Ollivon D. Atmospheric bulk deposition of PAHs onto France: trends from urban to remote sites. Atmos Environ 2002;36:5395–403.

Garty J. Biomonitoring atmospheric heavy metals with lichens: theory and application. Crit Rev Plant Sci 2004;20(4):309–71.

Gladtke D, Bakker F, Biaudet H, Brennfleck A, Coleman P, Creutznacher H, et al. Different collector types for sampling deposition of polycyclic aromatic hydrocarbons — comparison of measurement results and their uncertainty. J Environ Monit 2012;14:2054–62.

Gocht T, Klemm O, Grathwohl P. Long-term atmospheric bulk deposition of polycyclic aromatic hydrocarbons (PAHs) in rural areas of Southern Germany. Atmos Environ 2007;41:1315–27.

Golomb D, Ryan D, Eby N, Underhill J, Zemba S. Atmospheric deposition of toxics onto Massachusetts Bay — I. Metals. Atmos Environ 1997;31:1349–59.

Gunawardena J, Egodawatta P, Ayoko GA, Goonetilleke A. Atmospheric deposition as a source of heavy metals in urban stormwater. Atmos Environ 2013;68:235–42.

Halsall CJ, Coleman PJ, Jones KC. Atmospheric deposition of polychlorinated dibenzo-p-dioxins/dibenzofurans PCDD/Fs and polycyclic aromatic hydrocarbons PAHs in two UK cities. Chemosphere 1997;35(9):1919–31.

Hein FJ, Langenberg CW, Kidston C, Berhane H, Berezniuk T. A comprehensive field guide for facies characterization of the Athabasca Oil Sands, Northeast Alberta. Edmonton, Alberta: Alberta Energy and Utility Board, Alberta Geological Survey; 2001. [http://www.ags.gov.ab.ca/publications/abstracts/SPE_013.html, 2001 [June 11, 2013]].

Hoff RM, Strachan WMJ, Sweet CW, Chan CH, Shackleton M, Bidleman TF, et al. Atmospheric deposition of toxic chemicals to the Great Lakes: a review of data through 1994. Atmos Environ 1996;30:3505–27.

Hovmand MF, Kemp K, Kystol J, Johnsen I, Riis-Nielsen T, Pacyna JM. Atmospheric heavy metal deposition accumulated in rural forest soils of southern Scandinavia. Environ Pollut 2008;155:537–41.

Huang X, Olmez I, Aras NK, Gordon GE. Emissions of trace elements from motor vehicles: potential marker elements and source composition profile. Atmos Environ 1994;28:1385–91.

Huang C-J, Chen K-S, Lai Y-C, Wang L-C, Chang-Chien G-P. Characterization of atmospheric dry deposition of polychlorinated dibenzo-p-dioxins/dibenzofuran in a rural area of Taiwan. Aerosol Air Qual Res 2011;11:448–59.

Hughes WB, Holba AG, Dzou LIP. The ratios of dibenzothiophene to phenanthrene and pristine to phytane as indicators of depositional environment and lithology of petroleum source rocks. Geochim Cosmochim Acta 1995;59:3581–98.

International Standards Organization (ISO). Air quality-measurement of atmospheric dustfall — horizontal deposit gauge method. ISO/DIS 4222.2; 1979.

International Standards Organization (ISO). Air quality-guidelines for estimating measurement uncertainty. ISO 20988; 2007.

Jeffries DS, Snyder WR. Atmospheric deposition of heavy metals in central Ontario. Water Air Soil Pollut 1980;15:127–52.

Jervis RE, Richard Ho K-L, Tiefenbach B. Trace impurities in Canadian oil sands, coals and petroleum products and their fate during extraction, upgrading and combustion. J Radioanal Chem 1982;71:225–41.

Kelly EN, Schindler DW, Hodson PV, Short JW, Radmanovich R. Oil sands development contributes polycyclic aromatic compounds to the Athabasca River and its tributaries. Proc Natl Acad Sci U S A 2009;106:22346–51.

Kelly EN, Short JW, Schindler DW, Hodson PV, Ma M, Kwan AK, et al. Oil sands development contributes elements toxic at low concentrations to the Athabasca River and its tributaries. Proc Natl Acad Sci U S A 2010;107:16178–83.

Khalaf F, Literathy V, Anderlini V. Vanadium as a tracer of oil pollution in the sediments of Kuwait. Hydrobiologia 1982;91–92:147–51.

Kleinman MT, Eisenbud M, Lippman M, Kneip TJ. Use of tracers to identify sources of airborne particles. Environ Inter 1980;4:53–62.

Korhonen M, Kiviranta A, Ketola R. Bulk deposition of PAHs, PCBs and HCHs in Finland in summer seasons 1993–1996. Toxicol Environ Chem 1998;66(1–4):37–45.

Krachler M, Zheng J, Koerner R, Zdanowicz C, Fisher D, Shotyk W. Increasing atmospheric antimony contamination in the northern hemisphere: snow and ice evidence from Devon Island, Arctic Canada. J Environ Monit 2005;7:1169–76.

Kurek J, Kirk JL, Muir DCG, Wang X, Evans MS, Smol JP. Legacy of a half century of Athabasca oil sands development recorded by lake ecosystems. Proc Natl Acad Sci U S A 2013;110:1761–6.

Kyllönen K, Karlsson V, Ruoho-Airola T. Trace metal deposition and trends during a ten year period in Finland. Sci Total Environ 2009;407:2260–9.

Laflamme RE, Hites RA. The global distribution of polycyclic aromatic hydrocarbons in recent sediments. Geochim Cosmochim Acta 1978;42:289–303.

Landis MS, Pancras JP, Graney JR, Stevens RK, Percy KE, Krupa S. Receptor modeling of epiphytic lichens to elucidate the sources and spatial distribution of inorganic air pollution in the Athabasca Oil Sands Region. Dev Environ Sci 2012;11:427–67.

Leister D, Baker J. Atmospheric deposition of organic contaminants to the Chesapeake Bay. Atmos Environ 1994;28:1499–520.

Lian J-J, Li C-L, Ren Y, Cheng T-T, Chen J-M. Determination of alkyl polycyclic aromatic hydrocarbons in dustfall by supercritical fluid extraction followed by gas chromatography/mass spectrum. Bull Environ Contam Toxicol 2009;82:189–93.

Liu F, Xu Y, Liu J, Liu D, Li J, Zhang G, et al. Atmospheric deposition of polycyclic aromatic hydrocarbons (PAHs) to a coastal site of Hong Kong, South China. Atmos Environ 2013;69:265–72.

Lowenthal DH, Wittorff D, Gertler AW, Sakiyama S. CMB source apportionment during REVEAL. J Environ Eng 1997;123:80–7.

Mamane Y. Estimate of municipal refuse incinerator contribution to Philadelphia aerosol-I. Source analysis. Atmos Environ 1988;22:2411–8.

Manoli E, Samara C, Konstantinou I, Albanis T. Polycyclic aromatic hydrocarbons in the bulk precipitation and surface waters of Northern Greece. Chemosphere 2000;41:1845–55.

Mari M, Harrison RM, Schuhmacher M, Domingo JL, Pongpiachan S. Inference over the sources and processes affecting polycyclic aromatic hydrocarbons in the atmosphere derived from measured data. Sci Total Environ 2010;408:2387–93.

Menichini E, Barbera S, Merli F, Settimo G, Viviano G. Atmospheric bulk deposition of carcinogenic PAHs in a rural area in southern Italy. Polycycl Aromat Compd 2006;26:253–63.

Mijić Z, Stojiæ A, Perišiæ M, Rajšiæ S, Tasiæ M, Radenkoviæ M, et al. Seasonal variability and source apportionment of metals in the atmospheric deposition in Belgrade. Atmos Environ 2010;44:3630–7.

Mizohata A, Mamuro T. Chemical element balances and identification of air pollution sources in Sakai, Osaka (II). J Jpn Soc Air Pollut 1980;15:225–33.

Moon H-B, Kannan K, Lee S-J, Ok G. Atmospheric deposition of polycyclic aromatic hydrocarbons in an urban and a suburban area of Korea from 2002 to 2004. Arch Environ Contam Toxicol 2006;51:494–502.

Morrison KA, Kuhn ES, Watras CJ. Comparison of three methods of estimating atmospheric mercury deposition. Environ Sci Technol 1995;29:571–6.

Motelay-Massei A, Ollivon D, Tiphagne K, Garban B. Atmospheric bulk deposition of trace metals to the Seine river Basin, France: concentrations, sources and evolution from 1988 to 2001 in Paris. Water Air Soil Pollut 2005;164:119–35.

Motelay-Massei A, Ollivon D, Garban B, Tiphagne-Larcher K, Zimmerlin I, Chevreuil M. PAHs in the bulk atmospheric deposition of the Seine river basin: source identification and apportionment by ratios, multivariate statistical techniques and scanning electron microscopy. Chemosphere 2007;67:312–21.

Nicholson FA, Smith SR, Alloway BJ, Carlton-Smith C, Chambers BJ. An inventory of heavy metals inputs to agricultural soils in England and Wales. Sci Total Environ 2003;311:205–19.

Nriagu JO, Pacyna JM. Quantitative assessment of worldwide contamination of air, water and soils by trace metals. Nature 1988;333:134–9.

Oaki A, Uematsu M, Miura K, Nakae S. Sources of sodium in atmospheric fine particles. Atmos Environ 2002;36:4367–74.

Ollivon D, Blanchoud H, Motelay-Massei A, Garban B. Atmospheric deposition of PAHs to an urban site, Paris, France. Atmos Environ 2002;36:2891–900.

Ondov JM, Choquette CE, Zoller WH, Gordon GE, Biermann AH, Heft RE. Atmospheric behavior of trace elements on particles emitted from a coal-fired power plant. Atmos Environ 1989;23:2193–204.

Pacyna JM, Semb A, Hanseen JE. Emission and long-range transport of trace elements in Europe. Tellus 1984;36B:163–78.

Pacyna JM, Bartonova A, Cornille P, Mainhaut W. Modelling of long-range transport of trace elements: a case study. Atmos Environ 1989;23:107–14.

RGAR. United Kingdom Review Group on acid rain. Acid deposition in the United Kingdom 1981–1985. Stevenage: Warren Spring Laboratory; 1987.

Rossini P, Guerzoni S, Molinaroli E, Rampazzo G, De Lazzari A, Zancanaro A. Atmospheric bulk deposition to the lagoon of Venice part I. Fluxes of metals, nutrients and organic contaminants. Environ Inter 2005;31:959–74.
Rossini P, Matteucci G, Raccanelli S, Favotto M, Guerzoni S, Gattolin M. Polycyclic aromatic hydrocarbons in atmospheric depositions around the Venice lagoon. Polycycl Aromat Compd 2007;27(3):197–210.
Sanderson EG, Raqbi A, Vyskocil A, Farant JP. Comparison of particulate polycyclic aromatic hydrocarbon profiles in different regions of Canada. Atmos Environ 2004;38:3417–29.
Sawicki E. Analysis for airborne particulate hydrocarbons, their relative proportions as affected by different types of pollution. Monograph, 9. National Cancer Institute; 1962. p. 201–20.
Scheff PA, Valiozis C. Characterization and source identification of respirable particulate matter in Athens, Greece. Atmos Environ 1990;24:203–11.
Shaw RW. Air pollution by particles. Sci Am 1987;257:96–103.
Simó R, Grimalt JO, Albaigés J. Loss of unburned fuel hydrocarbons from combustion aerosols during atmospheric transport. Environ Sci Technol 1997;31:2697–700.
Sporstøl S, Rainer NG, Lichtenthaler RG, Gustavsen KO, Urdal K, Oreld F. Source identification of aromatic hydrocarbons in sediments using GC/MS. Environ Sci Technol 1983;17:282–6.
Staelens J, De Schrijver A, Van Avermaet P, Genouw G, Verhhoest N. A comparison of bulk and wet-only deposition at two adjacent sites in Melle (Belgium). Atmos Environ 2005;39:7–15.
Studabaker WB, Krupa S, Jayanty RKM, Raymer JH. Measurement of polynuclear aromatic hydrocarbons (PAHs) in epiphytic lichens for receptor modeling in the Athabasca Oil Sands Region (AOSR): a pilot study. Dev Environ Sci 2012;11:391–425.
Su Y, Wania F, Harner T, Lei YD. Deposition of polybrominated diphenyl ethers, polychlorinated biphenyls, and polycyclic aromatic hydrocarbons to a boreal deciduous forest. Environ Sci Technol 2007;41:534–40.
Tanner PA. Analysis of Hong Kong daily bulk and wet deposition data from 1994 to 1995. Atmos Environ 1999;33:1757–66.
Thurman HV. Introductory oceanography. 7th ed. Maxwell Macmillan, Canada, Inc.; 1994. p. 148.
United States Environmental Protection Agency (U.S. EPA). Sampling and analysis procedures for screening of industrial effluents for priority pollutants. Cincinnati: U.S. Environmental Protection Agency. Environment Monitoring and Support Laboratory; 1977.
Wakeham SG, Schaffner C, Geiger W. Polycyclic aromatic hydrocarbons in recent lake sediments—II. Compounds derived from biogenic precursors during early diagenesis. Geochim Cosmochim Acta 1980;44:415–29.
Wang W, Simonich SLM, Giri B, Xue M, Zhao J, Chen S, et al. Spatial distribution and seasonal variation of atmospheric bulk deposition of polycyclic aromatic hydrocarbons in Beijing Tianjin region, North China. Environ Pollut 2011;159:287–93.
Wayland M, Headley JV, Peru KM, Crosley R, Brownlee BG. Levels of polycyclic aromatic hydrocarbons and dibenzothiophenes in wetland sediments and aquatic insects in the oil sands area of Northeastern Alberta, Canada. Environ Monit Assess 2008;136:167–82.
Yunker MB, Snodon LR, Macdonald RW, Smith JN, Fowler MG, Skibo DN, et al. Polycyclic aromatic hydrocarbon composition and potential sources for sediment samples from the Beaufort and Barents Seas. Environ Sci Technol 1996;30:1310–20.
Yunker MB, Macdonald RW, Goyette D, Paton DW, Fowler BR, Sullivan D, et al. Natural and anthropogenic inputs of hydrocarbons to the Strait of Georgia. Sci Total Environ 1999;225:181–209.
Yunker MB, Macdonald RW, Vingarzan R, Mitchell RH, Goyette D, Sylvestre S. PAHs in the Fraser River basin: a critical appraisal of PAH ratios as indicators of PAH source and composition. Org Geochem 2002;33:489–515.
Zhang L, Gong SL, Padro J, Barrie L. A size-segregated particle dry deposition scheme for an atmospheric aerosol module. Atmos Environ 2001;35:549–60.
Zhang X, Siddiqi Z, Song X, Mandiwana KL, Yousaf M, Lu J. Atmospheric dry and wet deposition of mercury in Toronto. Atmos Environ 2012;50:60–5.